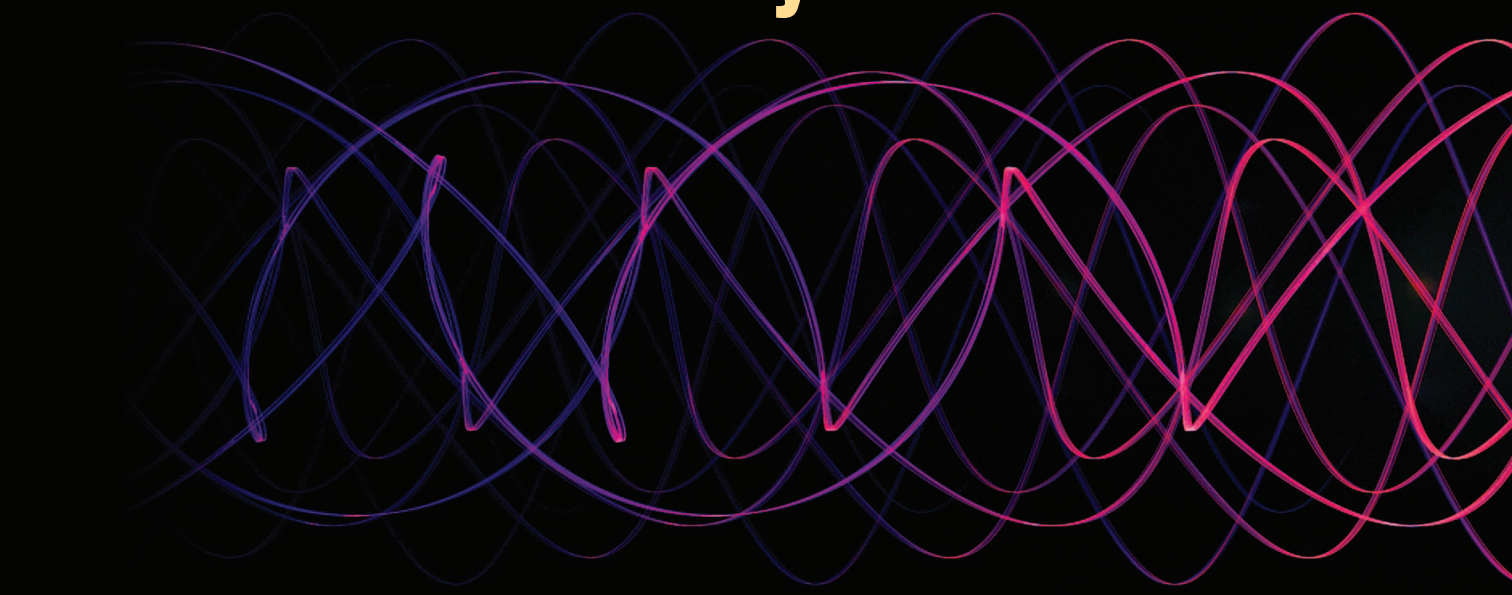
FIR Filter Design Using Optimal Factoring: A Walkthrough and Summary of Benefits



Alireza Mehrnia and Alan N. Willson, Jr.

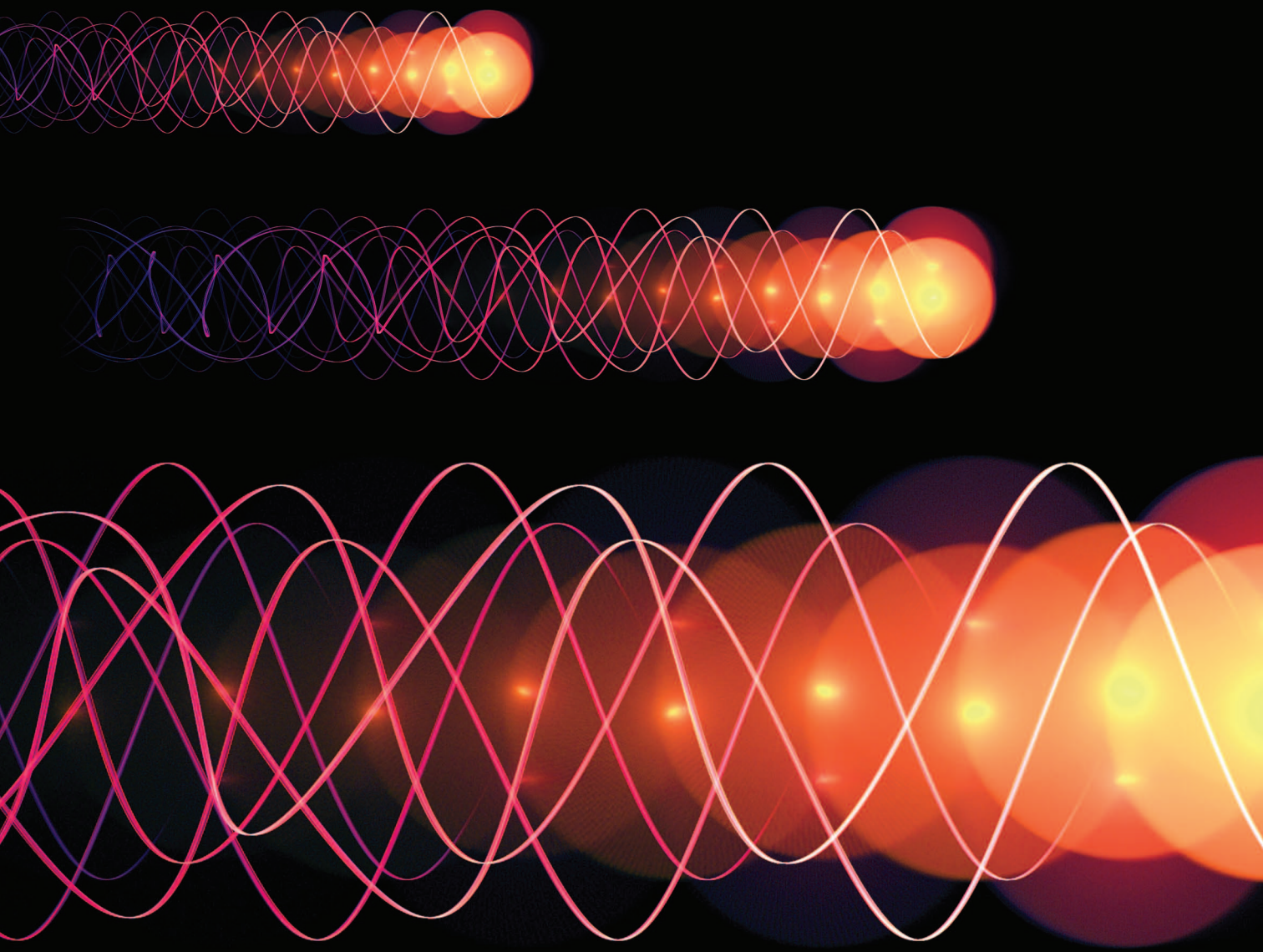
Abstract

Decomposing an FIR filter into a cascade of blocks, each representing an optimal factor of $H(z)$, the filter's transfer function, can start with the complex-conjugate pairs of zeros of $H(z)$ and then creating optimal pairings of these zero-pairs. This leads to a general method for designing FIR filters having minimal hardware complexity. We illustrate this concept, further techniques, benefits, and performance improvements in this paper, highlighting the practical features of the design method. It is also shown that the resulting structure can achieve lower hardware complexity, when compared with the prior art.

[1]The optimally-factored FIR filter design, method and structure are patent pending.

IMAGE LICENSED BY INGRAM PUBLISHING

Digital Object Identifier 10.1109/MCAS.2015.2510178
Date of publication: 12 February 2016



I. Introduction

The concept of realizing an FIR filter as a cascade of subfilters is found in some of the earliest signal processing publications [1, 2] and has long been viewed as a promising approach for building efficient digital filters [1-11]. At first the focus was on using *natural* (1st or 2nd degree) factors, most corresponding to one of the filter's complex-conjugate zero-pairs. Alternatives were then shown [3-10] to use a cascade of a prefilter and a second (magnitude equalizer) subfilter, or to use efficient identical subfilters, which could also be an effective technique in reducing a filter's coefficient sensitivity and hence, reducing its hardware complexity.

To achieve an even better (practical and hardware-efficient) realization of an FIR filter in the form of a cascade of sub-filters, an algorithm for the *optimal* factoring of FIR filter transfer functions was recently introduced [11] with a focus on creating factors based on *optimal pairings* of the natural zeros of the filter's transfer function. The approach also provides a systematic method to identify an optimal stage-*sequencing* for the cascade factors that minimizes hardware complexity.

In Section II of this paper, we showcase the optimal factoring[1] of an extensively cited FIR filter and, while doing so, we highlight various practical benefits of the new filter-design technique. We then demonstrate the flexibility of the factored structure by examining its

Alireza Mehrnia is with the Department of Electrical Engineering, University of California, Los Angeles, CA 90095 USA (e-mail: mehrnia@ucla.edu). Alan N. Willson, Jr. is the Charles P. Reames Research Professor at the Department of Electrical Engineering, University of California, Los Angeles, CA 90095 USA (e-mail: willson@ee.ucla.edu).

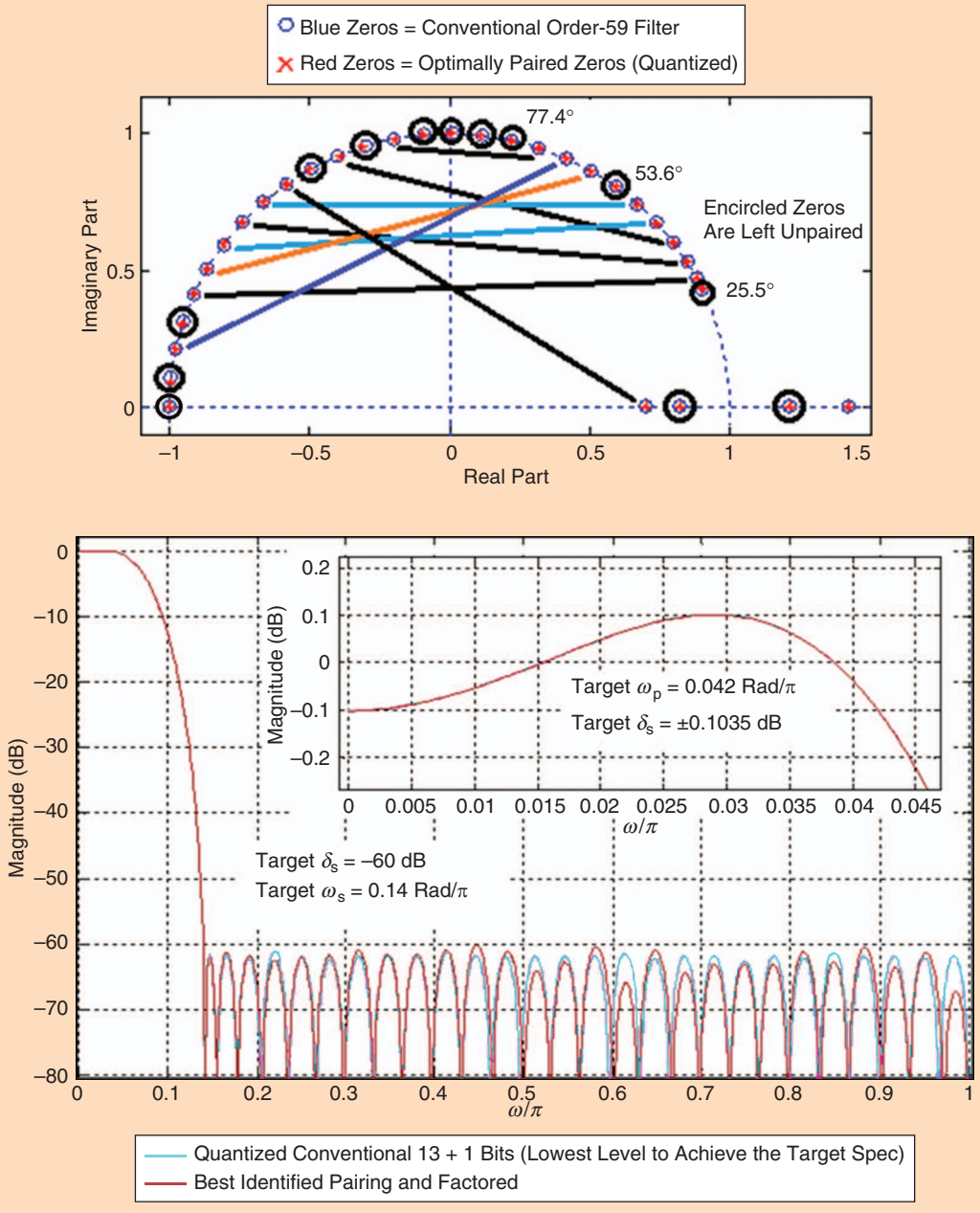


Figure 1. Zero maps, zero pairings and magnitude (dB) of optimally factored design vs. conventional implementation of order-59 filter example.

capability to adjust the filter's passband ripple by modifying specific factors while leaving the rest of the optimal factors untouched. In Section III we then examine, from a practical perspective, the resulting filter's performance. The achieved hardware complexity is also compared with previously published methods to show that the optimally-factored filter design achieves significantly lower hardware complexity than is found in the prior art.

II. Filter Design Via Optimal Factoring: A Walkthrough and Summary of Benefits

Consider the highly cited order-59 FIR filter [12] where:

Passband edge $\omega_p = 0.042\pi$ Stopband edge $\omega_s = 0.14\pi$
$\delta_p = 0.012\,(\pm 0.1035\,\text{dB})$ $\delta_s = 0.001\,(-60\,\text{dB})$.

This filter, also referred to in [13–19] as filter "S2," has been used to benchmark previous filter-design

To achieve an even better (practical and hardware-efficient) realization of an FIR filter in the form of a cascade of sub-filters, an algorithm for the optimal factoring of FIR filter transfer functions was recently introduced.

Table 1.
Decomposing the order-59 filter into its 30 natural quantized complex conjugate factors (no pairing of zero-pairs performed yet).

Factor	Non-Trivial Coef. (Binary)	Stage Shifter	Factor	Non-Trivial Coef. (Binary)	Stage Shifter
$1 + z^{-1}$	None	0.5	$1 - 1.47265625\ z^{-1} + z^{-2}$	1.01111001	2
$1 + z^{-2}$	None	0.5	$1 + 1.46875\ z^{-1} + z^{-2}$	1.01111	0.25
$1 - 0.1875\ z^{-1} + z^{-2}$	0.0011	0.5	$1 - 1.59765625\ z^{-1} + z^{-2}$	1.10011001	2
$1 + 0.234375\ z^{-1} + z^{-2}$	0.001111	0.5	$1 + 1.640625\ z^{-1} + z^{-2}$	1.101001	0.25
$1 + 0.359375\ z^{-1} + z^{-2}$	0.010111	0.5	$1 - 1.69921875\ z^{-1} + z^{-2}$	1.10110011	4
$1 - 0.419921875\ z^{-1} + z^{-2}$	0.011010111	0.5	$1 + 1.703125\ z^{-1} + z^{-2}$	1.101101	0.25
$1 + 0.625\ z^{-1} + z^{-2}$	0.101	0.5	$1 - 1.765625\ z^{-1} + z^{-2}$	1.110001	4
$1 - 0.625\ z^{-1} + z^{-2}$	0.101	1	$1 - 1.8056640625\ z^{-1} + z^{-2}$	1.1100111001	4
$1 + 0.8125\ z^{-1} + z^{-2}$	0.1101	0.5	$1 + 1.S359375\ z^{-1} + z^{-2}$	1.1101011	0.25
$1 - 0.828125\ z^{-1} + z^{-2}$	0.110101	1	$1 + 1.890625\ z^{-1} + z^{-2}$	1.111001	0.25
$1 + z^{-1} + z^{-2}$	None	0.25	$1 + 1.953125\ z^{-1} + z^{-2}$	1.111101	0.25
$1 - 1.015625\ z^{-1} + z^{-2}$	1.000001	1	$1 + 1.9921875\ z^{-1} + z^{-2}$	1.1111111	0.25
$1 - 1.171875\ z^{-1} + z^{-2}$	1.001011	1	$1 - 2.03759765625\ z^{-1} + z^{-2}$	10.00001001101	–32
$1 + 1.25\ z^{-1} + z^{-2}$	1.01	0.25	$1 - 2.1259765625\ z^{-1} + z^{-2}$	10.0010000001	–8
$1 + 1.25\ z^{-1} + z^{-2}$	1.01	0.25	Post-filter multiplier = β =	Post-filt-mult =	
$1 - 1.328125\ z^{-1} + z^{-2}$	1.010101	2	1.070983886718750	1.0001001000101	

approaches. Its Parks–McClellan (conventional) FIR realization has the zero map and magnitude response shown in Fig. 1. We decompose this conventional realization into its 30 natural factors, i.e., its 30 1st-order or 2nd-order factors (which have a total of 27 non-trivial coefficients [i.e., non-zero coefficients that are not an exact *power-of-two*]) as listed in Table 1. We then employ our optimal factoring algorithm [11] on this filter. The resulting optimal zero-pairings are shown in Fig. 1 (by straight lines touching paired zeroes). The magnitude response, and the zero map of the conventional canonic signed-digit (CSD) design [12] are also shown in Fig. 1. Notice that this filter has 27 complex-conjugate zero pairs on the unit-circle, one unit-circle zero at $z = -1$, and two sets of off-unit-circle zero pairs near $z = 1$. Binary representations of the non-trivial coefficients, also listed in Table 1, can be efficiently realized with 57 shift-add operations (multiplier adders) excluding the post-filter gain adjustment multiplier β. (By "shift-add" we mean a hard-wired shift and an addition.) The filter also has 58 structural adders and 59 registers.

For this example the optimal zero-pairing [11] arrives at the 21 factors listed in Table 2. The detailed properties of these factors, summarized in Table 2, illustrate (left columns) which natural factors from Table 1 are paired to obtain the optimal pairings shown in Fig. 1. As is explained in [11], the practical realization of a factored

Table 2.
Order-59 filter - optimally paired factors.

Optimally Factored Cascade				
Angle (Degrees)		**Quantized 21 Factors (Stages) (Outcome of Optimal Zero-Pairing)**	**Non-Trivial Coefs (Absolute Binary)**	**Stage Shifter**
180	1:	$1 + z^{-1}$	None	0.5
±90	2:	$1 + z^{-2}$	None	0.5
0(2)	3:	$1 - 2.0374755859375\ z^{-1} + z^{-2}$	10.0000100110011	–32
0(2), ±125	4:	$1 - 0.96484375\ z^{-1} - 0.46875\ z^{-2} - 0.96484375\ z^{-3} + z^{-4}$	[0.11110111 0.01111000]	–2
±25.5	5:	$1 - 1.8046875\ z^{-1} + z^{-2}$	1.1100111	4
±28, ±156	6:	$1 + 0.0546875\ z^{-1} - 1.21875\ z^{-2} + 0.0546875\ z^{-3} + z^{-4}$	[0.0000111 1.00111]	1
±32, ±137	7:	$1 - 0.21875\ z^{-1} - 0.5\ z^{-2} - 0.21875\ z^{-3} + z^{-4}$	[0.00111 None]	1
±37, ±113	8:	$1 - 0.8125\ z^{-1} + 0.75\ z^{-2} - 0.8125\ z^{-3} + z^{-4}$	[0.1101 0.1100]	1
±42, ±143	9:	$1 + 0.125\ z^{-1} - 0.375\ z^{-2} + 0.125\ z^{-3} + z^{-4}$	[None 0.011]	0.5
±48, ±132	10:	$1 - 0.015625\ z^{-1} + 0.21875\ z^{-2} - 0.015625\ z^{-3} + z^{-4}$	[0.000001 0.001110]	0.5
±53.6	11:	$1 - 1.1875\ z^{-1} + z^{-2}$	1.0011	1
±60, ±150	12:	$1 + 0.71875\ z^{-1} + 0.25\ z^{-2} + 0.71875\ z^{-3} + z^{-4}$	[0.10111 None]	0.5
±65, ±168	13:	$1 + 1.125\ z^{-1} + 0.375\ z^{-2} + 1.125\ z^{-3} + z^{-4}$	[1.001 0.011]	0.25
±71, ±101	14:	$1 - 0.25\ z^{-1} + 1.75\ z^{-2} - 0.25\ z^{-3} + z^{-4}$	[None 1.11]	0.25
±77.4	15:	$1 - 0.4375\ z^{-1} + z^{-2}$	0.0111	0.5
±83.7	16:	$1 - 0.21875\ z^{-1} + z^{-2}$	0.00111	0.5
±95.4	17:	$1 + 0.1875\ z^{-1} + z^{-2}$	0.0011	0.5
±108.2	18:	$1 + 0.625\ z^{-1} + z^{-2}$	0.101	0.5
±120	19:	$1 + z^{-1} + z^{-2}$	None	0.25
±162.4	20:	$1 + 1.90625\ z^{-1} + z^{-2}$	1.11101	0.25
±175	21:	$1 + 1.9921875\ z^{-1} + z^{-2}$	1.1111111	0.25
		Post-filter multiplier = β = 1.180419921875	Mult = 1.0010111000110	

$H(z)$ cascade requires a careful choice of stage sequencing so as to effectively manage the datapath wordlength through the cascade stages (to minimize hardware complexity). The best identified stage-sequence for this order-59 optimally-factored filter [11] (using stage numbers given in Table 2, Column 2) is:

13-10-8-6-14-9-4-12-17-7-11-20-15-3-21-16-2-5-19-18-1

The resulting optimally factored cascade structure for this order-59 filter $H(z)$ is shown in Fig. 2 (according to the above sequence.) Each stage is followed by its stage shifter (a power-of-two multiplier) and a truncation. The binary representations of the non-trivial coefficients are also listed in Table 2, which indicates that the optimally factored design can be implemented with 58 structural adders. It can also be inferred from Table 2 that 30 adders (multiplier adders) in the form of shift-add operations can realize all non-trivial coefficients. Therefore the Fig. 2 optimally factored cascade filter can be implemented with a total of 88 additions and 59 registers. Notice that, as shown in Fig. 1, while passband behaviors are almost identical, the stopband performance of the factored cascade implementation is slightly better than that of the CSD filter of [12]. The coefficients of this CSD filter are listed in the "Quantized coefficients" column of Table 3 which indicates that its direct-form implementation requires 57 multiplier-adders after subexpression sharing is applied (excluding the post-filter multiplier), 59 structural adders and 59 registers. Therefore, the direct form implementation of the

The operating speed of the filters in Fig. 2 can far exceed that of conventional (Remez) designs, in the same technology, due to the ease of inserting pipeline-registers between the cascaded factors.

order-59 CSD filter, requiring a total of 116 shift-adds (excluding the post-filter multiplier), as compared to the optimally-factored design's 88 shift-adds is seen to be a 24% reduction). (Benefit #1)

The comparisons of the coefficient quantization levels for the optimally factored structure vs. the order-59 CSD filter are presented in Table 3. According to the binary representation of coefficients in Table 3, the *average coefficient quantization level per stage* is less than 6 bits (excluding sign bit) for the proposed optimally factored truncated implementation vs. the 13 bits of the conventional CSD design listed in Table 3, indicating an *approximately 55% reduction*! (Benefit #2)

An additional benefit of the considerable flexibility of the optimally factored structure: *Adjusting the passband ripple of the filter by just modifying specific factors associated with the passband while leaving the rest of the optimal factors untouched.* (Benefit #3)

For this order-59 example, if the designer is allowed a small (less than 0.01 dB) increase in the Fig. 1 passband ripple (to ±0.1085 dB), then the fusion of factors #3 (having the costliest coefficient of Table 2) and #20 results in a new 4th-order factor having lower hardware complexity in comparison with the total for factors #3 and #20 (Stages #14 and #12 in Fig. 2), as illustrated in (1):

$$\begin{aligned}&\text{Conv}[1 - 2.0374755859375\,z^{-1} + z^{-2},\ 1 + 1.90625\,z^{-1} + z^{-2}]\\&= 1 - 0.1328125\,z^{-1} - 1.8828125\,z^{-2} - 0.1328125\,z^{-3} + z^{-4}\\&0.1328125 = (0.0010001)_2,\ 1.8828125 = (1.1110001)_2. \qquad (1)\end{aligned}$$

If the rest of the 19 factors remain intact, the resulting magnitude response for the (tamed) modified

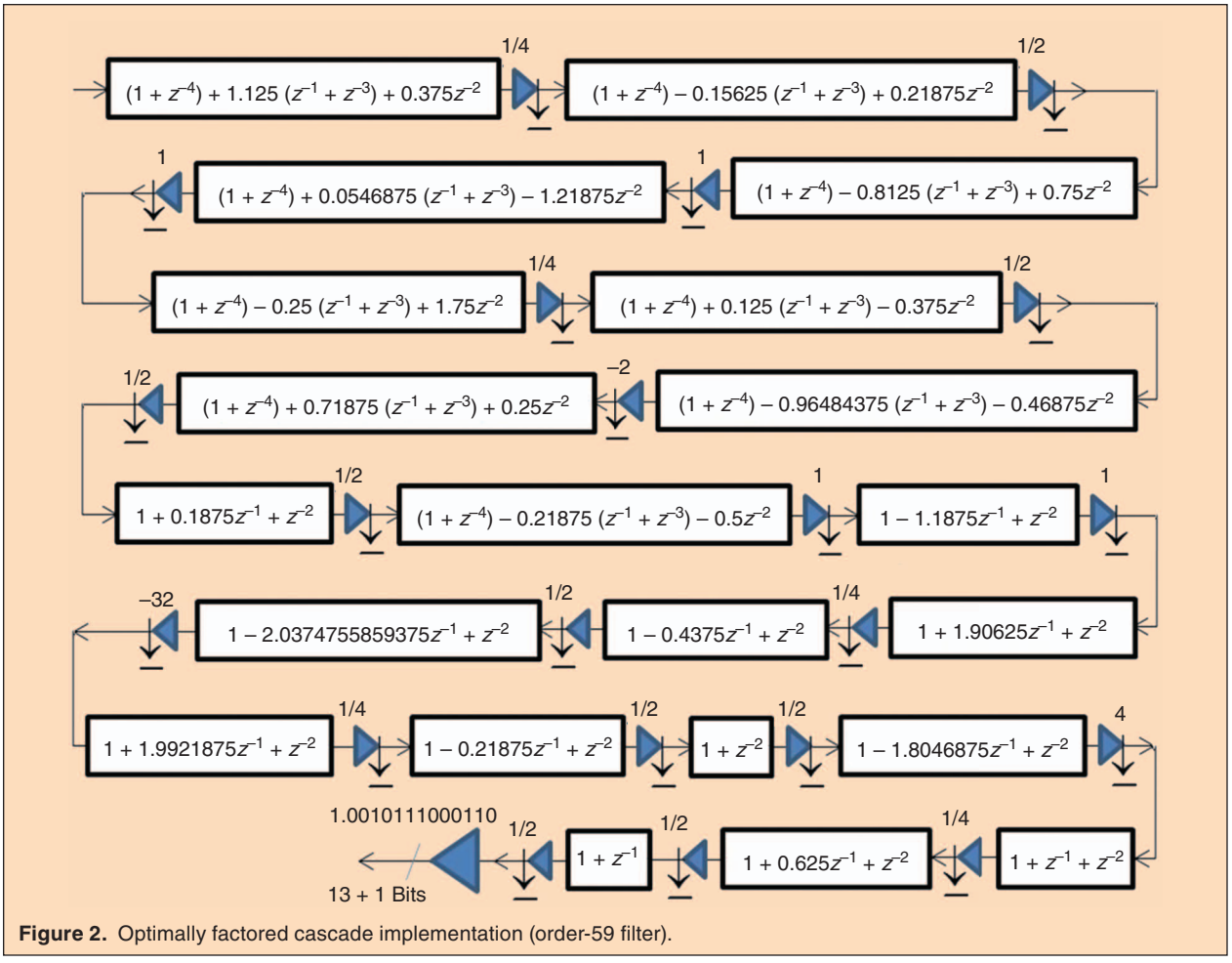


Figure 2. Optimally factored cascade implementation (order-59 filter).

Table 3.
Coefficient SPT for the optimally factored design vs. conventional Order-59 CSD design of [12].

Optimally Factored Design		Order-59 CSD Filter [12]
Coefficients (Abs Value)	**Signed Power-of-Two (SPT) terms**	**Quantized Coefficients Signed Power-of-Two (SPT) Terms**
None	None	$h(0) = 2^{-8} - 2^{-13}$
None	None	$h(1) = 2^{-8} - 2^{-11}$
10.0000100110011	$2 + 2^{-5} + (2^{-8} + 2^{-9})(1 + 2^{-4})$	$h(2) = 2^{-8} - 2^{-11} + 2^{-13}$
[0.11110111 0.01111]	$[1 - 2^{-5} - 2^{-8} \quad 2^{-1} - 2^{-5}]$	$h(3) = 2^{-9} - 2^{-11} + 2^{-12}$
1.1100111	$(2 - 2^{-2})(1 + 2^{-5})$	$h(4) = 2^{-10}$
[0.0000111 1.00111]	$[2^{-4} - 2^{-7} \quad 1 + 2^{-2} - 2^{-5}]$	$h(5) = -2^{-9} - 2^{-13}$
[0.00111 0.1]	$[2^{-2} - 2^{-5} \quad 2^{-1}$	$h(6) = -2^{-7} + 2^{-11} + 2^{-13}$
[0.1101 0.11]	$[2^{-1} + 2^{-2} + 2^{-4} \quad 2^{-1} + 2^{-2}]$	$h(7) = -2^{-6} + 2^{-9} + 2^{-11}$
[0.001 0.011]	$[2^{-3} \quad 2^{-2} + 2^{-3}]$	$h(8) = -2^{-6} - 2^{-7} + 2^{-11}$
[0.000001 0.00111]	$[2^{-6} \quad 2^{-2} - 2^{-5}]$	$h(9) = -2^{-5} - 2^{-9} + 2^{-11}$
1.0011	$1 + 2^{-3} + 2^{-4}$	$h(10) = -2^{-4} + 2^{-6} + 2^{-8}$
[0.10111 0.01]	$[2^{-1} + 2^{-2} - 2^{-5} \quad 2^{-2}]$	$h(11) = -2^{-4} + 2^{-7} + 2^{-9}$
[1.001 0.011]	$[1 + 2^{-3} \quad 2^{-2} + 2^{-3}]$	$h(12) = -2^{-4} + 2^{-10} + 2^{-11}$
[0.01 1.11]	$[2^{-2} \quad 2 - 2^{-2}]$	$h(13) = -2^{-4} - 2^{-9} - 2^{-11}$
0.0111	$2^{-1} - 2^{-4}$	$h(14) = -2^{-4} - 2^{-9} - 2^{-13}$
0.00111	$2^{-2} - 2^{-5}$	$h(15) = -2^{-4} + 2^{-7} - 2^{-9}$
0.0011	$2^{-3} + 2^{-4}$	$h(16) = -2^{-5} - 2^{-7} + 2^{-9}$
0.101	$2^{-1} + 2^{-3}$	$h(17) = -2^{-6} - 2^{-13}$
1	1	$h(18) = 2^{-6} + 2^{-8} - 2^{-12}$
1.11101	$2 - 2^{-3} + 2^{-5}$	$h(19) = 2^{-4} + 2^{-9} - 2^{-12}$
1.1111111	$2 - 2^{-7}$	$h(20) = 2^{-3} - 2^{-7} + 2^{-11}$
		$h(21) = 2^{-3} + 2^{-4} - 2^{-7}$
		$h(22) = 2^{-2} - 2^{-8} - 2^{-10}$
		$h(23) = 2^{-2} + 2^{-4} + 2^{-9}$
		$h(24) = 2^{-1} - 2^{-3} + 2^{-7}$
		$h(25) = 2^{-1} - 2^{-4} + 2^{-7}$
		$h(26) = 2^{-1} + 2^{-9} - 2^{-12}$
		$h(27) = 2^{-1} + 2^{-5} + 2^{-6} - 2^{-12}$
		$h(28) = 2^{-1} + 2^{-4} + 2^{-6} + 2^{-13}$
		$h(29) = 2^{-1} + 2^{-4} + 2^{-5} + 2^{-11}$
		$h(n) = h(59 - n)$, for $n = 30, 31, \ldots, 59$

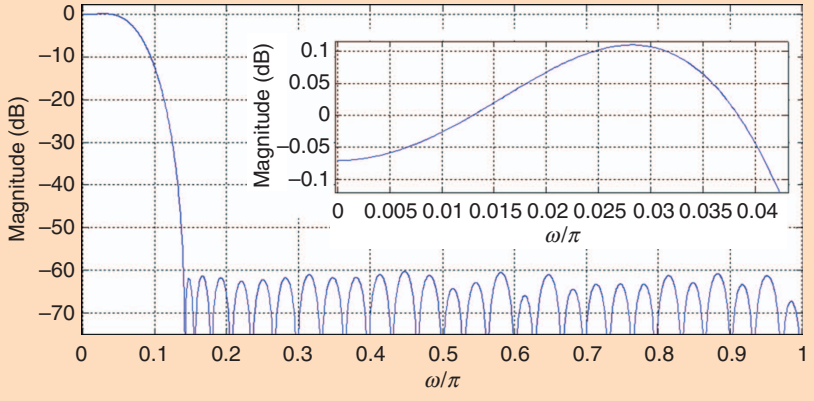


Figure 3. Magnitude (dB) of modified factored cascade obtained by fusing factor #3 and factor #20 from Table 2. (order-59 filter example).

factored cascade, shown in Fig. 3, has a passband ripple that is limited to ±0.1085 dB and a stopband attenuation that is *better than* the required 60-dB specification.

The resulting 4th-order factor in (1) has two non-trivial coefficients that require only (8+1)-bit quantization, compared to the (15+1)-bit quantization of factor #3 and (6+1)-bit quantization of factor #20, according to Table 2. The number of shift-add operations needed to implement the resulting 4th-order factor is less than the non-fused case by three shift-adds.

An additional benefit of the considerable flexibility of the optimally factored structure is that adjusting the passband ripple of the filter can be made by just modifying specific factors associated with the passband while leaving the rest of the optimal factors untouched.

The magnitude response of the new 4th-order factor (1) is plotted in Fig. 4 and it shows that the frequency domain behavior of factor #3 (red dashed line) is considerably tamed (i.e., it has less out-of-band gain) when it is fused (convolved) with factor #20 (blue dashed line). Hence, we also refer to this as a "cascade taming" technique. Given that the fusion of the aforementioned factors results in the removal of two 2nd-order factors and the introduction of the new 4th-order factor (1), the total number of cascade factors is reduced by one. Thus we require a re-examination of the stage sequencing for the modified cascade. We employed the sequencing algorithm described in [11] for the 20 factors. The revised optimally factored structure is shown in Fig. 5. The new 4th-order factor is highlighted in red. The green dashed line indicates the

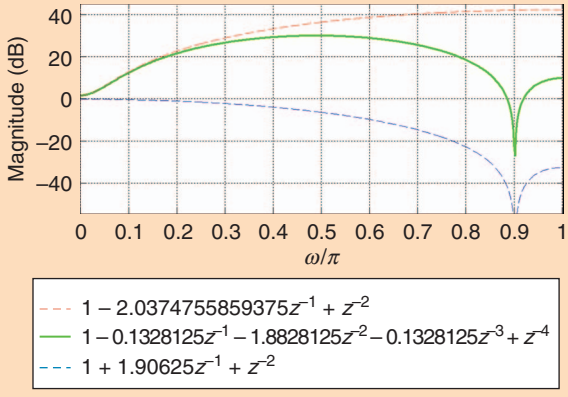


Figure 4. Magnitude (dB) of factor #3 and factor #20 from Table 2 and the resulting tamed 4th-order factor according to (1).

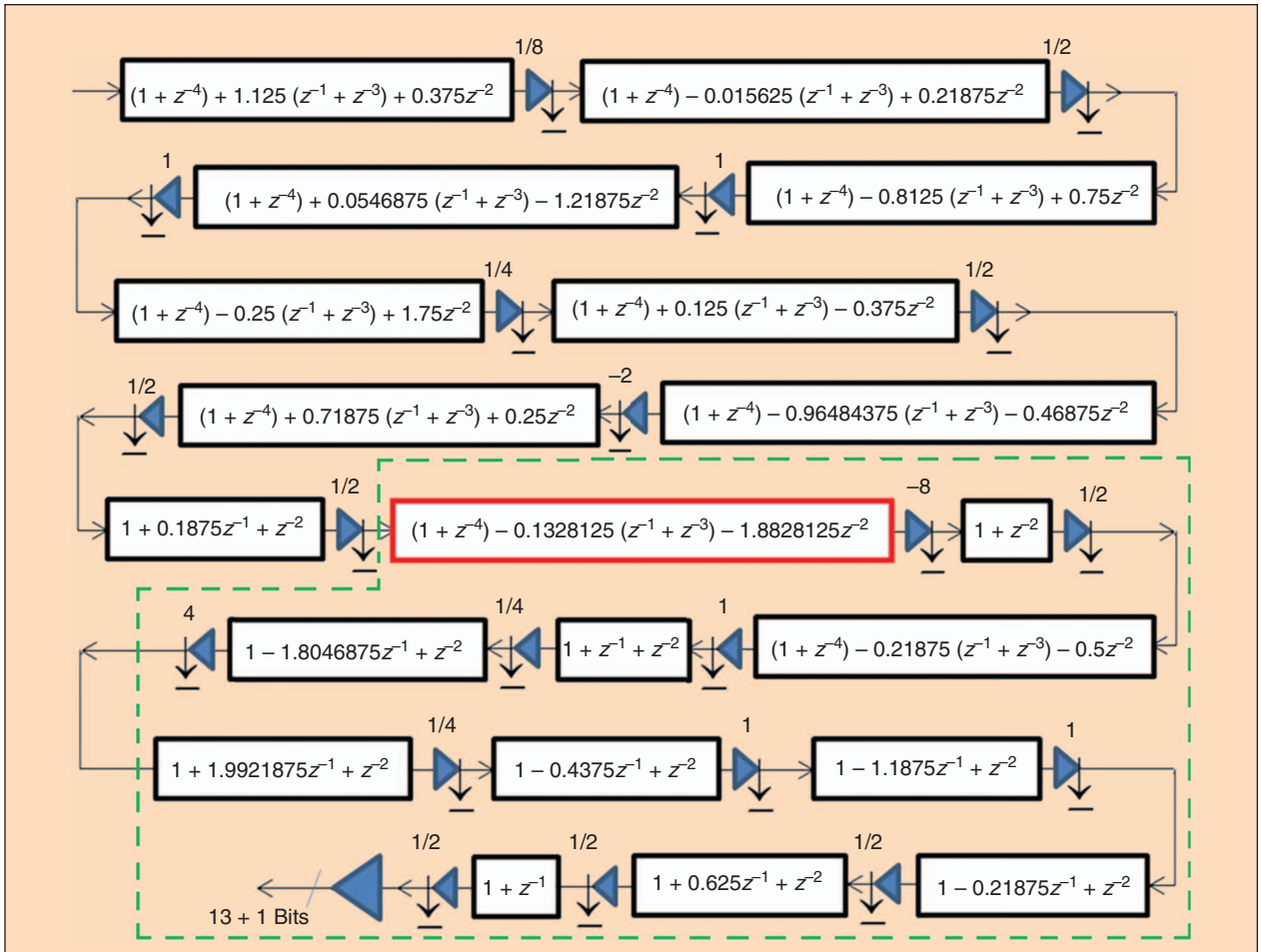


Figure 5. Tamed optimally factored structure - red border shows resulting stage after fusing two 2nd order factors described in (1) (order-59 filter).

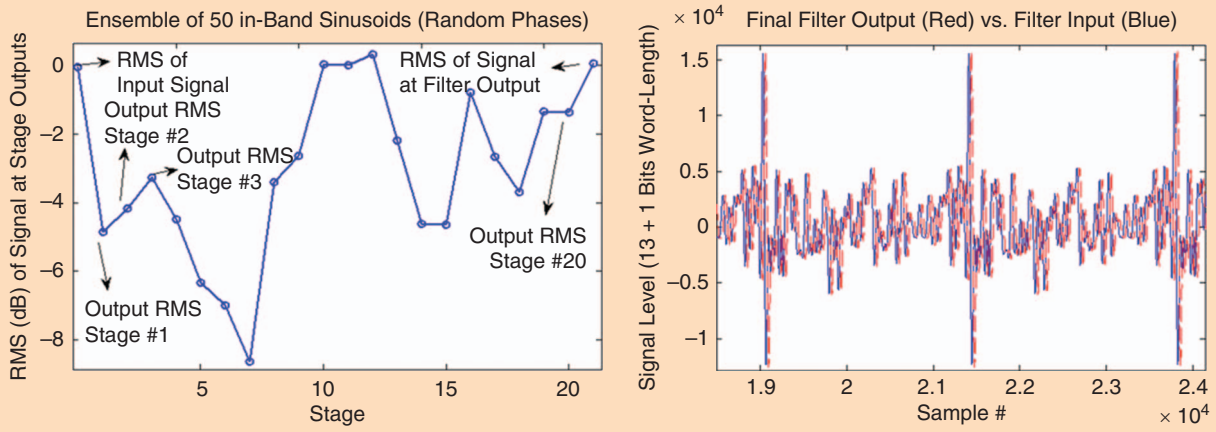


Figure 6. RMS of stage outputs in the modified factored cascade in Fig. 5 for Test 1 (ensemble of 50 in-band sinusoids).

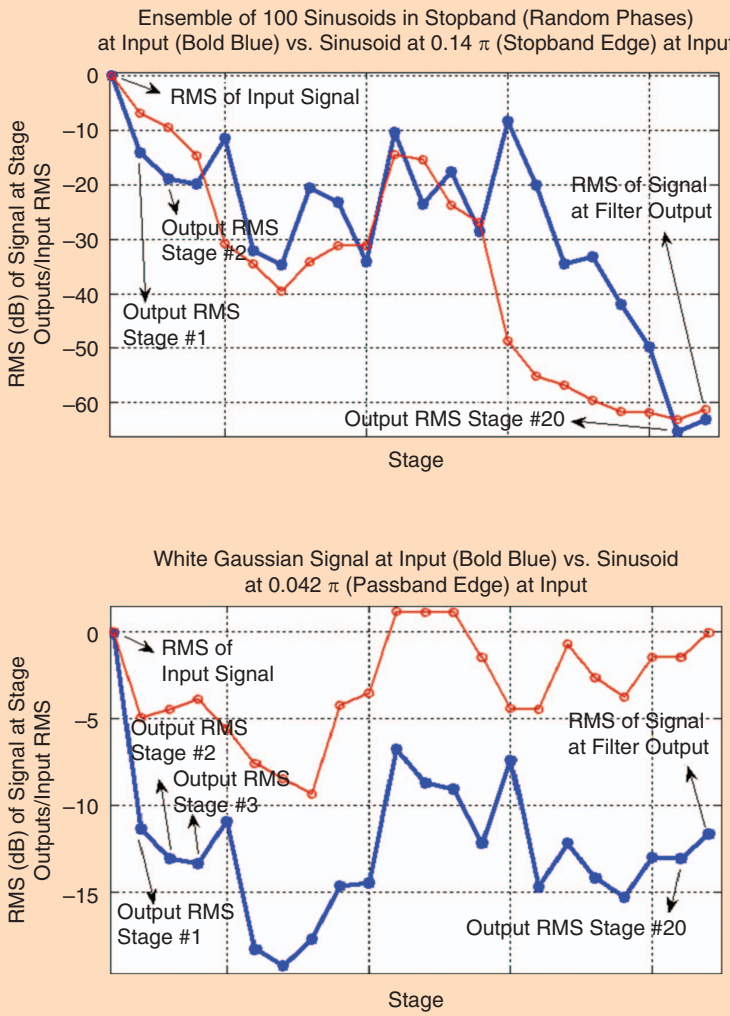


Figure 7. RMS of stage outputs in the modified factored cascade of Fig. 5 for Test 1 (ensemble of sinusoids).

portion of the cascade where the stage ordering has changed (from that of the original Fig. 2 cascade).

Easy Pipelining: Notice that both *partial* and *fully pipelined* versions of the factored Fig. 5 structure can easily be realized by simply inserting registers (buffers) between adjacent stages. This streamlined and straightforward pipelining is yet a further benefit of the optimally-factored structure. (Benefit #4)

III. Performance and Hardware Complexity

To examine the effectiveness of the stage sequencing, as implemented in the Fig. 5 *modified* factored cascade, we use the following comprehensive tests and measure the output RMS values for all 20 cascade stages.

- Test 1: the input signal is an ensemble of 50 in-band sinusoids (random phases). We expect the signal to traverse the factored filter unaffected and the output to be a delayed version of the input.
- Test 2: the input signal is white Gaussian noise (uniform power across all frequencies). We expect our filter to attenuate the portion of the signal that falls within the stopband ($\omega_s \geq 0.14\pi$) by 60 dB.

- Test 3: the input signal is a colored Gaussian noise signal with uniform power only in the stopband. We realized this using a sum of 100 random-phase sinusoids, uniformly distributed in the stopband. We expect our filter to attenuate the entire signal by at least 60 dB.
- Test 4: the input signal is a sinusoid at the passband edge ($\omega_p = 0.042\pi$).
- Test 5: the input signal is a sinusoid at the stopband edge ($\omega_s = 0.14\pi$).

The input signal RMS is set at $2^{N-1.5}$ for all cases (allowing in this example a margin of 1.5-bit for signal variations above the RMS level). Parameter N is the truncation level (wordlength of the signal) excluding the sign bit. Given the desired 60 dB attenuation, the wordlength (N), excluding sign bit, should be at least 13 bits for the modified factored cascade with $M = 20$ stages and 11 bits for the conventional single-stage design.

The results of the aforementioned Tests and the corresponding sequence of signal RMS values at the output of the stages are shown in Fig. 6 for Test 1 and, Fig. 7 for Tests 2, 3, 4 and 5. Fig. 6 shows that for Test 1 the filter output has the same RMS level as the filter input (left plot) and the time domain output signal (in red) shown in the right plot is a delayed version of the input signal (delayed by 29.5 samples since the filter order is 59). Fig. 7 shows the RMS of the output signals of the 20 stages of the factored structure in Fig. 5 for Tests 2 and 3 (bold blue), 4 and 5 (red). As shown in the top plot, the output signal is fully attenuated by at least 60 dB for Tests 3 and 5 where the input signal contains only stopband content. The bottom plot in Fig. 7 illustrates that the sinusoid at the edge of the passband (red) has the same RMS level at both the filter's input and output. It also shows (bold blue) that, when the input signal has uniform power spectral density, the filter attenuates the stopband portion ($\omega \geq 0.14\pi$) by at least 60 dB; hence the power of the filter's output signal is reduced by approximately 12 dB in comparison with that of the White Gaussian input signal.

Noise analysis for the modified factored structure: We now examine the noise performance of the optimally factored structure of Fig. 5. The truncation events at the outputs of the $M = 20$ cascaded stages inject quantization noise into the data stream throughout the modified factored filter. These truncation events can be modeled by

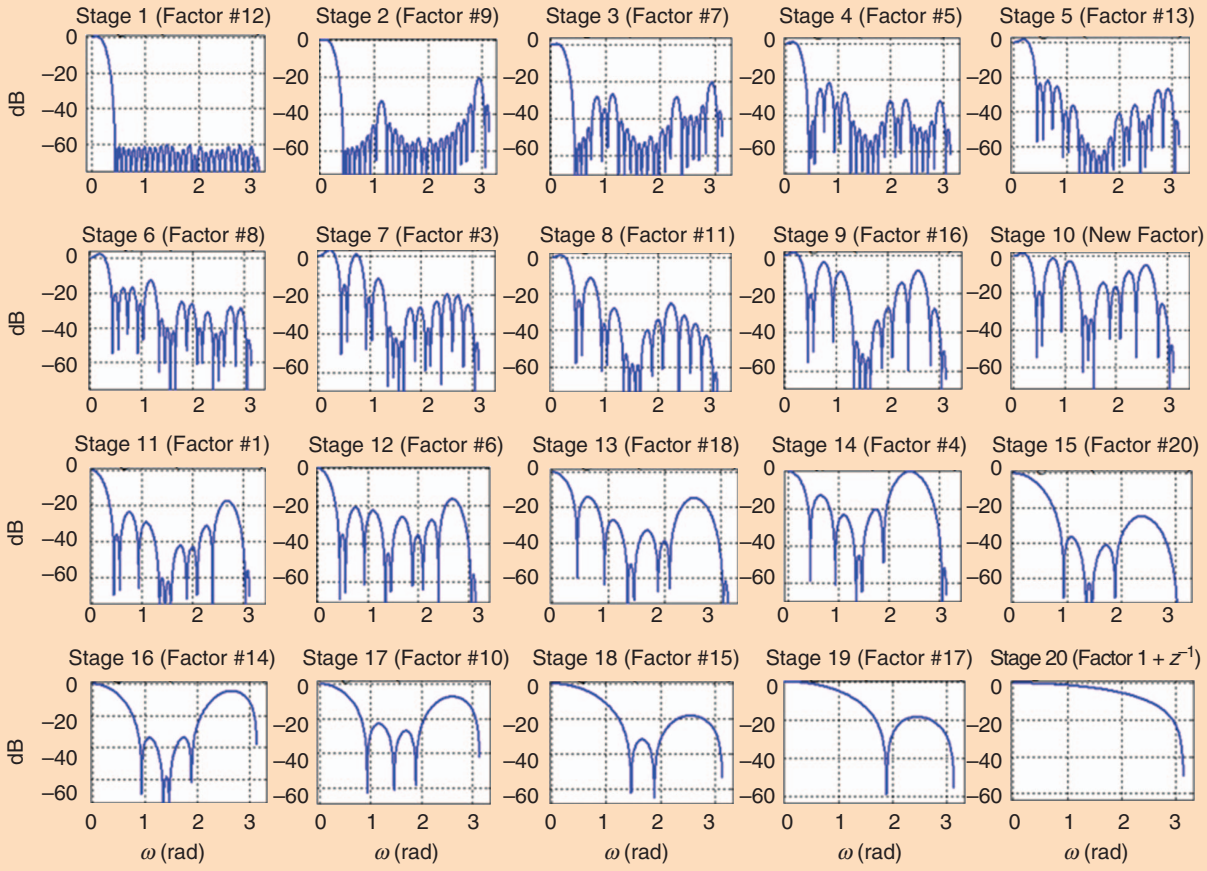


Figure 8. Effective total magnitude (dB) that each of 20 noise sources experiences from the point of truncation to the output of the Fig. 5 structure.

M independent and identically distributed (i.i.d.) additive uniform noise sources at the output of the stages. Fig. 8 shows the effective total magnitude response (dB) that each of the *M* noise sources experiences, from the point of truncation noise insertion to the output of the Fig. 5 filter. Also, the overall effect of all 20 noise sources (from all cascade stages) at the filter output is shown in Fig. 9, where the bottom two plots are the histogram and the normalized PSD of the total noise at the output of the modified factored filter. The top plot is the RMS of total

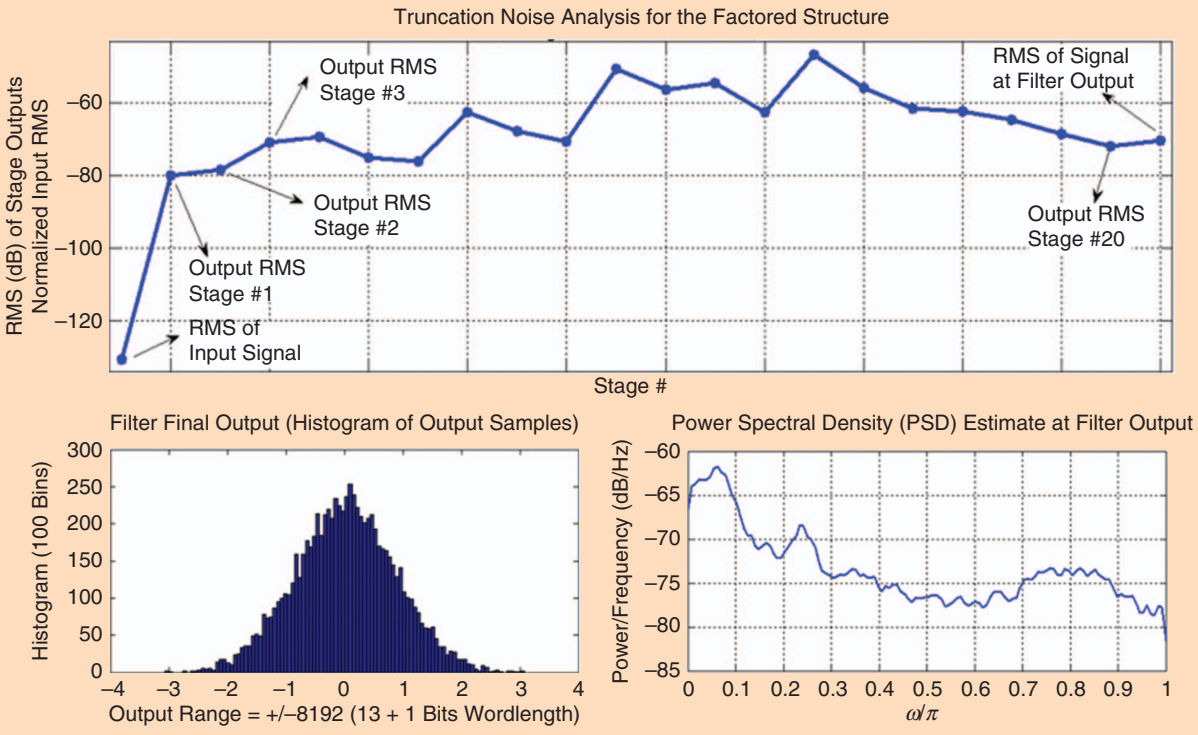


Figure 9. Overall effect of noise from all stages at the output of the modified factored cascade.

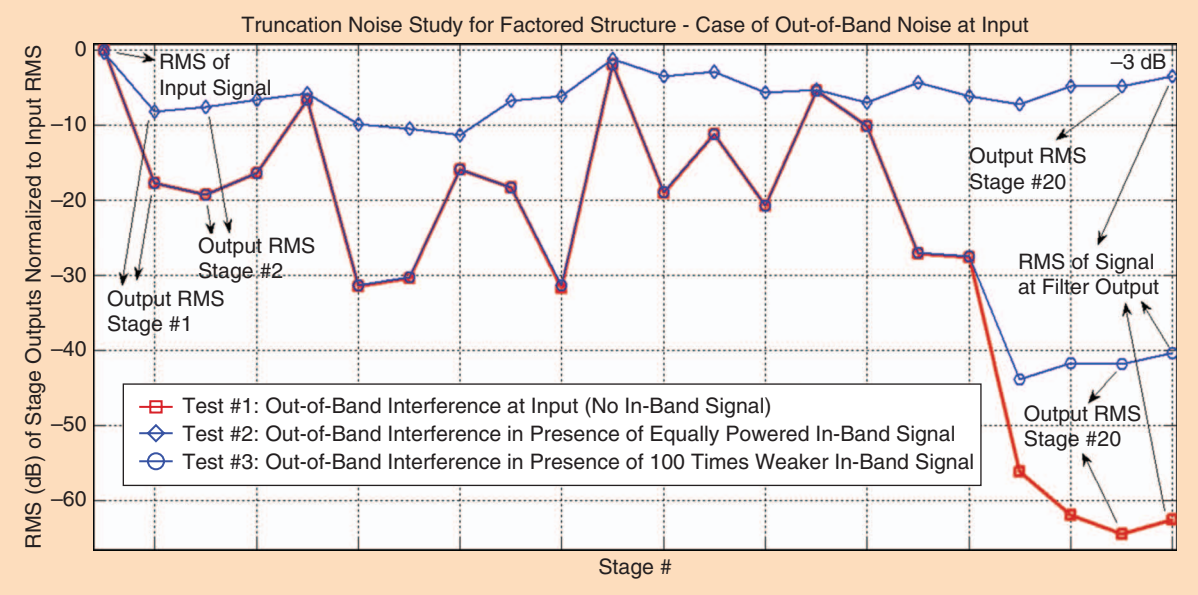


Figure 10. Interference test results for the sequenced, modified structure (Fig. 5).

TABLE 4.
Hardware complexity comparison for order-59 narrowband FIR filter (*B* represents the wordlength of the datapath) MA ≡ Multiplier Adders, SA ≡ Structral Adders.

Hardware Complexity for Alternative Filter Design Methods Data Wordlength = *B* bits	MA	SA	Total # of Adders	Full Adders (FA)	D Flip-Flops (FF)	Total Complexity (FA + FF)
Modified optimally factored (Fig. 5) Ripple = ± 0.1085 dB filter order = 59	27	58	85	1203 (*B* = 13 + 1 bits)	834 1103 for fully pipelined case	**2037** full pipelined: **2306** (*B* = 13 + 1 bits)
Optimally factored filter order = 59 Fig. 2 (*B* = 13 + 1 bits)	30	58	88	1270 (*B* = 13 + 1 bits)	842 1128 for fully pipelined ease	**2112** full pipelined: **2398** (*B* = 13 + 1 bits)
Genetic algorithm [18] Two-stage cascade filter order = 60	13	56	69	Our estimate: >1500 (*B* = 12)	Our estimate: >1300 (*B* = 12)	Our estimate: > **2800** (*B* = 11 + 1 bits)
Two-stage cascade [17] filter order = 59	14	55	69	697 + 69B [17] = 1525 (*B* = 12)	Our estimate: >1300 (*B* = 12)	Our estimate: >**2825** (*B* = 12)
MILP method [15–16] filter order = 59	19	59	78	Our estimate: > 1600 (*B* = 12)	Our estimate: >135O (*B* = 12)	Our estimate: > **2950** (*B* = 12)
Single-stage design filter order = 59 [16]	17	59	76	729 + 76*B* [17] = 1641 (*B* = 12)	Our estimate: >135O (*B* = 12)	Our estimate: > **2991** (*B* = 12)
FIRGAM [13] filter order = 59	27	59	86	Our estimate: 1680 (*B* = 12) 1337 if *B* = 8 [13]	Our estimate: >141O (*B* = 12) 1180 if *B* = 8 [13]	Our estimate: > **3090** (*B* = 12)
PMILP [14], [13] filter order = 59	25	59	84	Our estimate: 1678 (*B* = 12) 1342 if *B* = 8 [13]	Our estimate: >1490 (*B* = 12) 1255 if *B* = 8 [13]	Our estimate: > **3168** (*B* = 12)
CSD [12], [13] filter order = 59	32	59	91	Our estimate: 1819 (*B* = 12) 1455 if *B* = 8 [13]	Our estimate: >1500 (*B* = 12) 1298 if *B* = 8 [13]	Our estimate: > **3319** (*B* = 12)
Remez [13] filter order = 59	32	59	91	Our estimate: 1858 (*B* = 12) 1494 if *B* = 8 [13]	Our estimate: >1480 (*B* = 12) 1251 if *B* = 8 [13]	Our estimate: > **3338** (*B* = 12)

noise at the output of each stage (taking into account all noise contributions from preceding stages in the cascade). Fig. 9 shows that the overall output noise in the stopband is well below the target -60 dB level that the filter is required to achieve.

Performance study for the modified factored structure – case of out-of band interference (blocker) at input: We have investigated various practical cases of out-of-band interference scenarios at the input in order to further illustrate the performance of the (13+1)-bit truncated modified cascade of Fig. 5. The results are summarized in Fig. 10 for the following three tests:

- Test 1: out-of-band interference between 0.3π and 0.4π (with no in-band signal). The filter is expected to fully attenuate the input to at least -60 dB at the output.
- Test 2: out-of-band interference (0.3π-0.4π) has the same power as the desired in-band signal. The filter is expected to remove interference (half of the input power), resulting in -3-dB output power relative to 0-dB input power.
- Test 3: out-of-band interference (0.3π-0.4π) has 40-dB higher power than the desired in-band signal. The filter is expected to remove the interference,

A practical hardware-efficient filter structure is realizable by decomposing an FIR filter into its natural factors, corresponding to the transfer function zeros, and constructing a more efficient factored cascade structure based on an optimal pairing of these natural factors.

resulting in approximately –40-dB power at the output relative to the input power level.

Fig. 10 confirms the satisfactory removal of the input out-of-band interference for Tests 2 and 3, leaving only the desired signal at the filter output with –3-dB and –40-dB power levels, respectively, relative to the input power. It also confirms the attenuation of out-of-band interference to the –62-dB level at the filter output for Test 1 (with no in-band (desired) signal at the input).

Hardware complexity of the modified factored structure: A comparison with eight published prior methods of implementing the order-59 filter is given in Table 4. Parameter B is the datapath word-length (and the truncation level in the factored design) which should be at least 11 bits (excluding sign bit) for the conventional single-stage designs so that they can provide enough resolution to be able, in practice, to realize the target 60-dB stopband attenuation. Parameter MA (multiplier adders) is the total number of adders that are required to implement coefficients of the filter. Parameter SA (structural adders) is the total number of all the remaining adders that are needed to realize the filter structure. The subject of optimal architectures for filter multipliers has been extensively investigated in the literature (e.g., [19, 20]) and is beyond the scope of this paper. Table 4 demonstrates that the proposed optimally factored structures in Fig. 5 and Fig. 2 have the lowest complexities, when compared with: the Genetic algorithm filter design [18], both single-stage and two-stage designs in [16] and [17], the MILP method [15], both FIRGAM and Remez implementations [13], the PMILP technique [14] and the CSD design [12]. The comparison is provided in terms of the sum of the total number of full adders (FA) and the total number of flip-flops (FF) that are used to realize the filter. This is believed to be the most comprehensive simple measure of an FIR filter's hardware complexity.

As a single simple measure of the improvement level provided by the optimally-factored filters: consider the complexity reduction relative to the Remez-based design in Table 4. It can be seen from Table 4 as: (3338 – 2112)/3338 = 36.7% and, when fully pipelined, (3338 – 2398)/3338 = 28.2%. (When fully pipelined, optimally-factored filters can be used at high speeds that cannot be reached by conventional direct-form filters.)

IV. Conclusion

A design walkthrough and summary of features and benefits have been presented in this paper for the recently announced optimal factoring method for FIR filter design. It is shown that a practical hardware-efficient filter structure is realizable by decomposing an FIR filter into its natural factors, corresponding to the transfer function zeros, and constructing a more efficient factored cascade structure based on an optimal pairing of these natural factors. Further features and benefits of the proposed filter-design method have also been highlighted including reduced coefficient quantization levels and reduced hardware complexity, ease of pipelining, flexibility to modify or fuse stages, and the capability to adjust the filter's passband ripple by modifying specific factors while leaving the rest of the cascade factors untouched. Results suggest that the optimally factored filter implementation has the potential to serve as a practical method to realize FIR filters with minimal hardware complexity and also easily facilitate new practical features that are not available when using a conventional filter design method.



Alireza Mehrnia received his Ph.D. degree in electrical engineering from UCLA with a focus on Wireless Integrated Circuits and Systems in 2006. He also received the M.B.A. degree from the UCLA Anderson School of Management in 2013 with a focus on Technology Strategy, Business Analytics and Management Consulting. He received the M.S.EE degree from Sharif University in 1998. From 2003 to 2009, he was the Director of RF Communications and a Founding engineer at WiLinx Inc., designing the first 3-10 GHz CMOS Giga-bit/s wireless transceiver system based on the Multi-Band OFDM UWB (Ultra Wideband) standard (IEEE 802.15.3a). He also represented the company from 2004 to 2009 in the UWB global standardization organization (WiMedia Alliance) and was the Lead Consultant in response to the Bluetooth board of directors' request for a feasibility study of MB-OFDM UWB-based WPAN (and wireless USB) data rate and range. Throughout this work, he contributed to the development of the Physical Layer and Architecture of the first Giga-bit/s commercial wireless standard as an active member, technical author

and later as the interim chairman of the worldwide UWB regulation. From 1998 to 2001, he worked with Kavoshcom (KCR) and PRI R&D, CA, as a team leader working on the design of system and baseband of a low power 12-satellite GPS receiver for mobile applications. Dr. Mehrnia holds 15 granted or pending patents and is the recipient of the UCLA Edward K. Rice outstanding engineering doctoral graduate of the year 2006 and the best paper award from ACM PADS, 2004. He has more than 10 years of experience in high-tech industry with a focus on RF and digital communications, signal processing, wireless integrated circuits and systems. He has also taught engineering courses at UCLA.



Alan N. Willson, Jr. (S'66–M'67–SM'73–F'78) received the B.E.E. degree from the Georgia Institute of Technology, Atlanta, in 1961, and the M.S. and Ph.D. degrees from Syracuse University, Syracuse, NY, in 1965 and 1967, respectively. From 1961 to 1964, he was with IBM, Poughkeepsie, NY. He was an Instructor in electrical engineering at Syracuse University from 1965 to 1967. From 1967 to 1973, he was a Member of the Technical Staff at Bell Laboratories, Murray Hill, NJ. Since 1973, he has been a member of the faculty at the University of California, Los Angeles (UCLA), where he is the Charles P. Reames Professor in the Department of Electrical Engineering. In addition, he served the UCLA School of Engineering and Applied Science as Associate Dean of Engineering from 1987 to 2001. In 1991 he founded Pentomics, Inc. He has been engaged in research concerning computer-aided circuit analysis and design, the stability of distributed circuits, properties of nonlinear networks, theory of active circuits, digital signal processing, analog circuit fault diagnosis, and integrated circuits for signal processing. He is the Editor of *Nonlinear Networks: Theory and Analysis* (IEEE Press, 1974). Dr. Willson is a member of the National Academy of Engineering, the Society for Industrial and Applied Mathematics, the American Society for Engineering Education, Eta Kappa Nu, Sigma Xi and Tau Beta Pi. From 1977 to 1979, he served as the Editor of the IEEE Transactions on Circuits and Systems. In 1980, he was the General Chairman of the 14th Asilomar Conference on Circuits, Systems, and Computers. During 1984, he served as the President of the IEEE Circuits and Systems Society. He was the recipient of the 1978 and 1994 Guillemin–Cauer Awards of the IEEE Circuits and Systems Society, the 1982 George Westinghouse Award of the American Society for Engineering Education, the 1982 Distinguished Faculty Award of the UCLA Engineering Alumni Association, the 1984 Myril B. Reed Best Paper Award of the Midwest Symposium on Circuits and Systems, the 1985 and 1994 W.R.G. Baker Awards of the IEEE, the 2000 Technical Achievement Award, and the 2003 Mac Van Valkenburg Award of the IEEE Circuits and Systems Society. He was the 2010 recipient of the IEEE Leon K. Kirchmayer Graduate Teaching Award, the 2013 Lockheed-Martin Award for Excellence in Teaching at UCLA, and the 2013 Vitold Belevitch Award of the IEEE Circuits and Systems Society.

References

[1] W. Schüssler, "On structures for nonrecursive digital filters," *Arch. Elek. Übertragung*, vol. 26, no. 6, pp. 255–258, June 1972.

[2] D. S. K. Chan and L. R. Rabiner, "An algorithm for minimizing round-off noise in cascade realizations of finite impulse response digital filters," *Bell Syst. Tech. J.*, vol. 52, no. 3, pp. 347–385, Mar. 1973.

[3] S. Nakamura and S. K. Mitra, "Design of FIR digital filters using tapped cascaded FIR subfilters," *Circuits Syst. Signal Processing*, vol. 1, no. 1, pp. 43–56, 1982.

[4] J. W. Adams and A. N. Willson, Jr., "A new approach to FIR digital filters with fewer multipliers and reduced sensitivity," *IEEE Trans. Circuits Syst.*, vol. CAS-30, no. 5, pp. 277–283, May 1983.

[5] J. W. Adams and A. N. Willson, Jr., "Some efficient digital prefilter structures," *IEEE Trans. Circuits Syst.*, vol. CAS-31, no. 3, pp. 260–266, Mar. 1984.

[6] P. P. Vaidyanathan and G. Beitman, "On prefilters for digital FIR filter design," *IEEE Trans. Circuits Syst.*, vol. CAS-32, no. 5, pp. 494–499, 1985.

[7] J. C. E. Cabezas and P. S. R. Diniz, "FIR filters using interpolated prefilters and equalizers," *IEEE Trans. Circuits Syst.*, vol. 37, no. 1, pp. 17–23, 1990.

[8] A. N. Willson, Jr., "Desensitized half-band filters," *IEEE Trans. Circuits Syst. I*, vol. 57, no. 1, pp. 152–165, Jan. 2010.

[9] A. Mehrnia and A. N. Willson, Jr., "Further desensitized FIR half-band filters," *IEEE Trans. Circuits Syst. I*, vol. 62, no. 7, July 2015.

[10] A. Mehrnia, M. Dai, and A. N. Willson, Jr., "Efficient halfband FIR filter structures for RF and IF data converters," *IEEE Trans. Circuits Syst. II*, vol. 63, no. 1, pp. 64–68, Jan. 2016.

[11] A. Mehrnia and A. N. Willson, Jr., "Optimal factoring of FIR filters," *IEEE Trans. Signal Process.*, vol. 63, no. 3, pp. 647–661, Feb. 2015.

[12] H. Samueli, "An improved search algorithm for the design of multiplierless FIR filters with powers-of-two coefficients," *IEEE Trans. Circuits Syst.*, vol. 36, no. 7, pp. 1044–1047, July 1989.

[13] M. Aktan, A. Yurdakul, and G. Dündar, "An algorithm for the design of low-power hardware-efficient FIR filters," *IEEE Trans. Circuits Syst. I*, vol. 55, no. 6, pp. 1536–1545, July 2008.

[14] C.-Y. Yao and C.-J. Chien, "A partial MILP algorithm for the design of linear phase FIR filters with SPT coefficients," *IEICE Trans. Fundam.*, vol. E85-A, pp. 2302–2310. Oct. 2002.

[15] Y. J. Yu and Y. C. Lim, "Design of linear phase FIR filters in subexpression space using mixed integer linear programming," *IEEE Trans. Circuits Syst. I*, vol. 54, no. 10, pp. 2330–2338, Oct. 2007.

[16] D. Shi and Y. J. Yu, "Design of linear phase FIR filters with high probability of achieving minimum number of adders," *IEEE Trans. Circuits Syst. I*, vol. 58, no. 1, pp. 126–136, Jan. 2011.

[17] D. Shi and Y. J. Yu, "Design of discrete-valued linear phase FIR filters in cascade form," *IEEE Trans. Circuits Syst. I*, vol. 58, no. 7, pp. 1627–1636, July 2011.

[18] W. B. Ye and Y. J. Yu, "Single-stage and cascade design of high order multiplierless linear phase FIR filters using genetic algorithm," *IEEE Trans. Circuits Syst. I*, vol. 60, pp. 2987–2997, Nov. 2013.

[19] A. G. Dempster and M. D. Macleod, "Use of minimum-adder multiplier blocks in FIR digital filters," *IEEE Trans. Circuits Syst. II Analog Digit. Signal Process.*, no. 9, pp. 569–577, Sept. 1995.

[20] A. Y. Kwentus, H. Hung, and A. N. Willson, Jr., "An architecture for high-performance/small-area multipliers for use in digital filtering applications," *IEEE J. Solid-State Circuits*, vol. 29, no. 2, pp. 117–121, Feb. 1994.